Proc. Schl. Eng. Tokai Univ., Ser. E
30 (2005) 7 - 14

Flow Characteristics and Pattern of Main Nozzle of Air Jet Loom

by

Chamlong Prabkeao[*1] and Katsumi Aoki[*2]

(Received on March 31, 2005 & Accepted on October 18, 2005)

Abstract

In this study, the flow characteristics and pattern of the main nozzle of an air jet loom were investigated experimentally. The static pressure and weft traction force of an acceleration tube with several main nozzles were measured. Moreover, the flow velocity and turbulence were measured on the basis of the laser doppler velocity (LDV). To clarify the flow pattern in the acceleration tube, visualization was performed by the spark tracing method.

Keywords: Flow characteristics, Jet loom, Laser doppler velocity, Spark tracing method, Visualization

1. Introduction

In recent years, the weft motion of weaving machines in textile manufacturing has been extensively transferred to the air jet loom, which can weave cloth of various yarns quickly. Discussions on the air jet loom usually take account of stalling velocity that occurs for an air flow which diffuses very rapidly. Up to now, some investigations on improvements, such as using an air guide and subnozzle [1-2] and changing the acceleration tube length and the air tank pressure [3-4], have been reported. However, the effect of the needle's shape on the flow pattern and the recirculation zone which develops in the mixing process has never been discussed.

In this paper, we describe the efficiency of the main nozzle with respect to the flow pattern inside the main nozzle and the acceleration tube. We examine the change in flow in the main nozzle that accompanies the change of the needle shape under the condition of a constant area ratio, referring to the measured static pressure and the weft traction force distribution. An expansion model was used to measure the velocity and turbulence distribution in the area where the recirculation zone occurs during the acceleration by the LDV. Moreover, visualization by the spark tracing method was carried out to clarify the flow pattern along the acceleration tube, and to examine the influence of the needle shape on the flow inside.

2. Experimental method

2.1 Structure and specifications of the main nozzle

Figure 1 shows the outline of the main nozzle used for this experiment, which is composed of the body, the needle and the acceleration tube. The structure of the needle is shown in figure 2, and table 1 lists its specifications. The guide passage, with a 2.8 mm diameter, is provided in the center of the needle, and the tip part has a tapered shape. Model No. 1 is a standard model. The others (model No. 2 ~ model No. 6) were made under the conditions of a constant area ratio decreasing 1 mm increments. Model No. 7 is extended 2 mm compared with model No. 1. Twelve measuring holes are provided for static pressure measurement in the body of the main nozzle and the acceleration tube, as figure 1 shows.

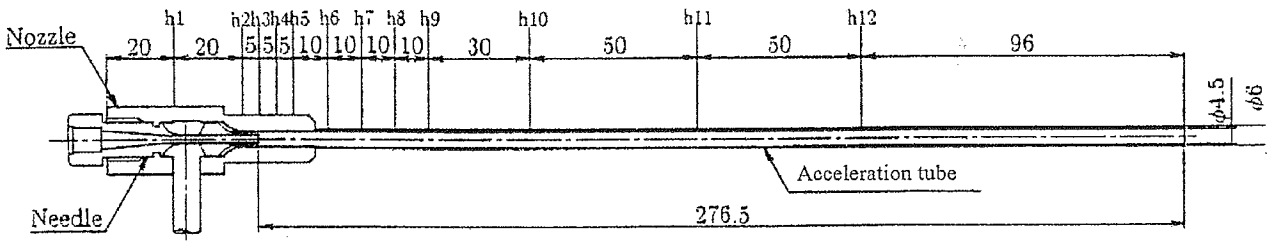

Fig. 1 Main nozzle and measuring points

*1 Associate Professor, Department of Mechanical Engineering, Faculty of Engineering, King Mongkuts Institute of Technology, Ladkrabang (KMITL), Bangkok, Thailand
*2 Professor, Department of Mechanical Engineering

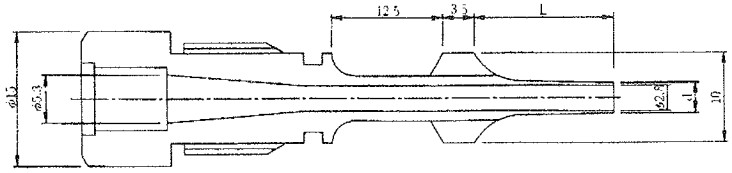

Fig. 2 Structure of needle

Table 1 Specifications of needle

Model No.	L [mm]	d [mm]	Throat area [mm^2]	Throat area ratio m
1	14.0	3.40	15.90	1.108
2	13.0	3.58		
3	12.0	3.76		
4	11.0	3.94		
5	10.0	4.11		
6	9.0	4.28		
7	16.0	3.40		

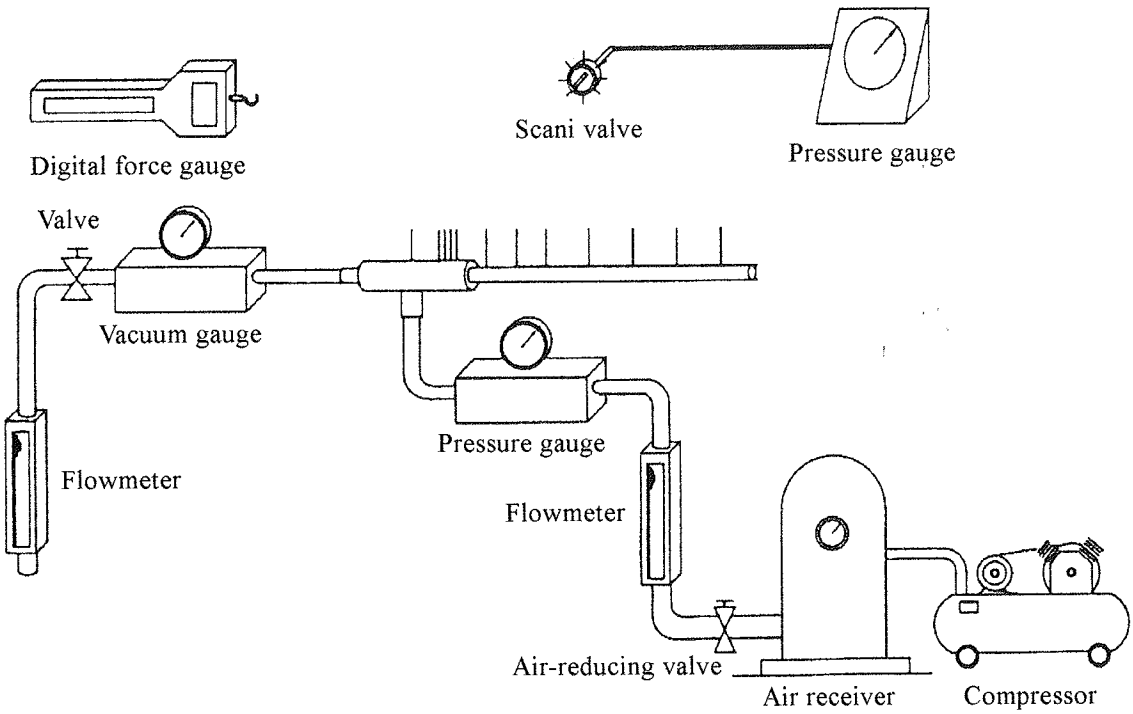

Fig. 3 Experimental apparatus (Pressure)

2.2 Measurement of static pressure and weft traction force

A schematic of the experiment of equipment is shown in figure 3. Air is supplied to the main nozzle by the compressor which applied a constant pressure to the main nozzle through the air receiver, filter and regulator. The static pressure is measured by a precise elastically shaped pressure gauge through the scani valve. The measurement is carried out applying a tank pressure between 2 kgf/cm^2 to 6 kgf/cm^2. The weft traction force is measured using digital force in the same equipment and under the same conditions as for static pressure measurement. The yarn length is 400 mm and the end of the yarn is in the acceleration tube exit.

2.3 Velocity measurement and visualization

A schematic for velocity measurement is shown in figure 4. The body is magnified 4.44 times by the main nozzle and the acceleration tube is made of acrylic resin to enable velocity measurement using LDV. The water is used as the medium in the acceleration tube, with the Reynolds number fixed at *Re*=14000. Figure 5 shows the measurement position of the velocity in the acceleration tube. At the axial distance x/D= 0.5~3.0, the interval of measurement is 0.25, and along x/D= 3.0~6.0 the interval is 1.0. Along the radial distance, the interval is 0.1 between r/R= -0.75~0.75. The flow pattern along the acceleration tube was visualized by the spark tracing method. In the experiment, we use a train of five pulses with a pulse interval of 50μs.

3. Results and discussion

3.1 Static pressure and Mach number distribution

To calculate the Mach number from the static pressure, the area is divided into 3 regions, as shown in figure 6, and flow is considered to be one-dimensional [3]. The region upstream of the main nozzles from the entrance of compressed air generated by the compressor at the inlet of the nozzle body to the needle tip is region A, the

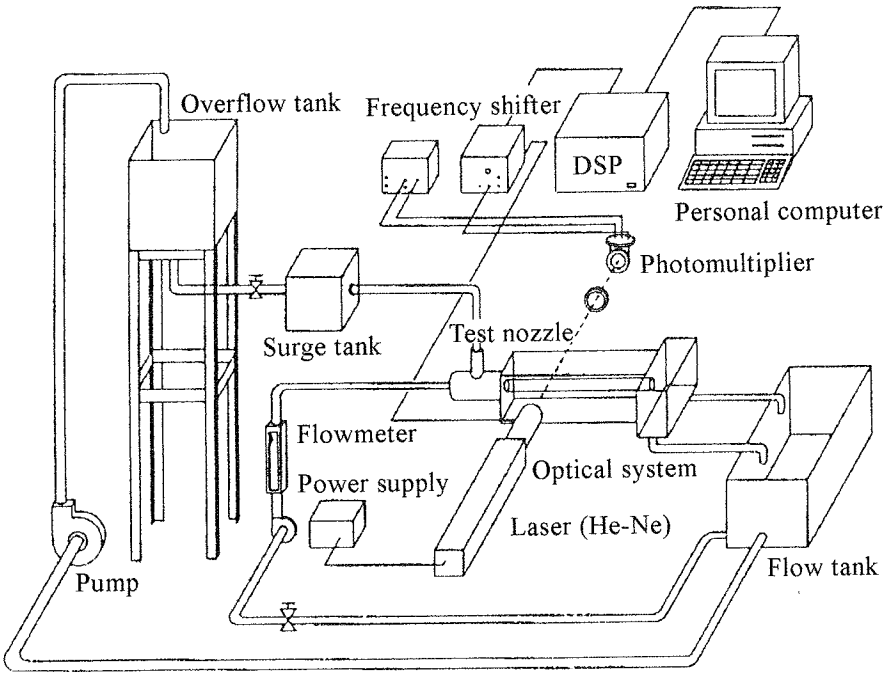

Fig. 4 Experimental apparatus (LDV)

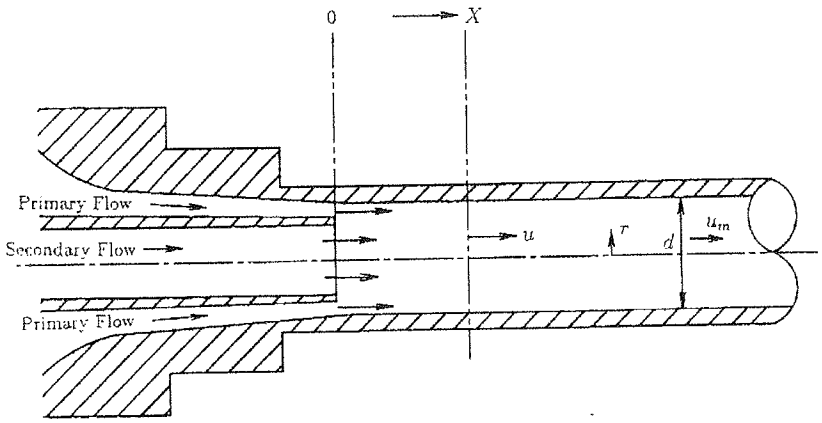

Fig. 5 Measurement point of velocity

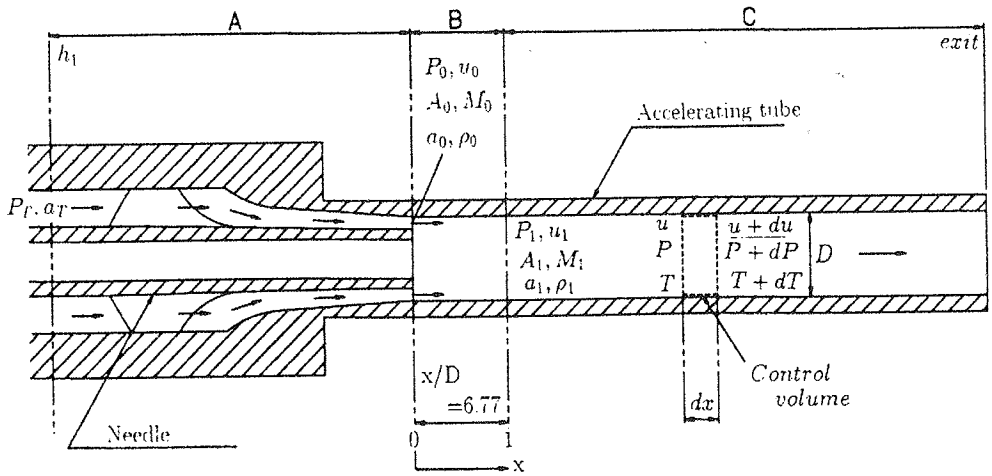

Fig. 6 Flow classification

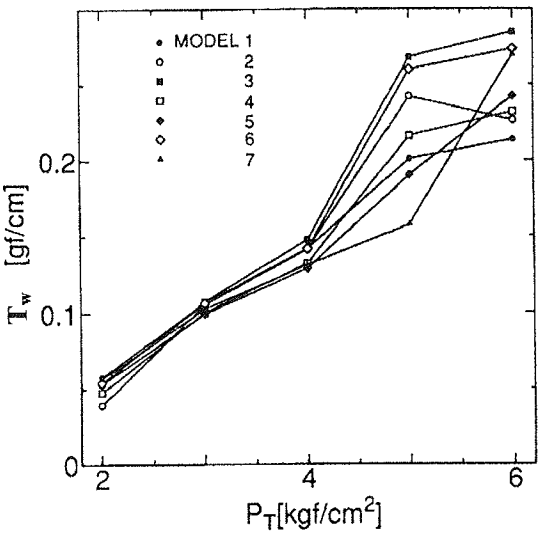

Fig. 7 Weft traction force

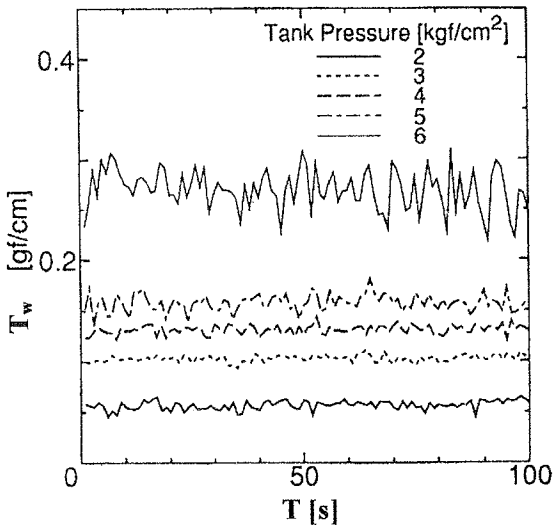

Fig. 8 Weft traction distribution

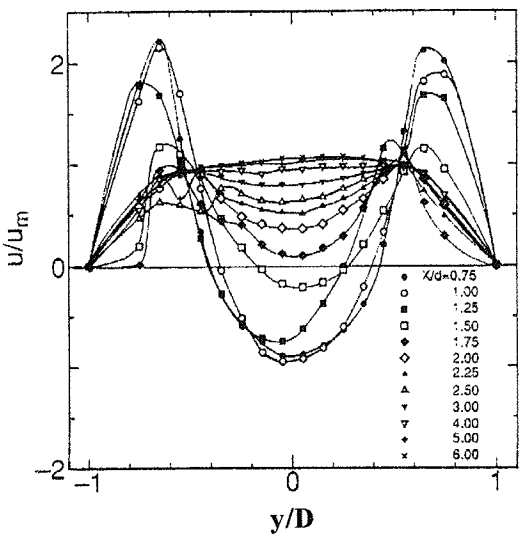

Fig. 9 Velocity distribution (*Re*=14000)

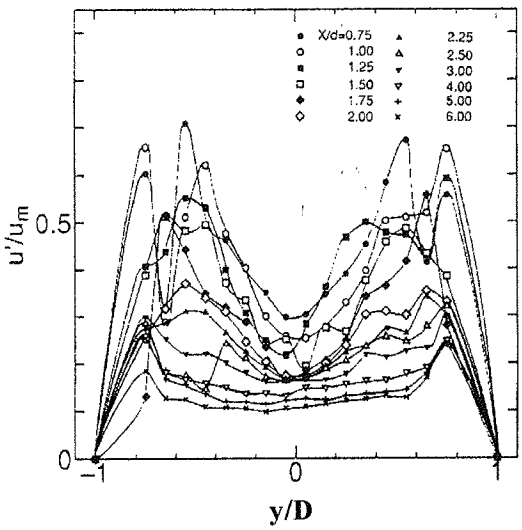

Fig. 10 Turbulence distribution (*Re*=14000)

expansion region is region B, and the area from the uniformly mixed point to the nozzle exit is region C. Flow in each region is calculated using the following formulas.

Flow in Region A:

$$\frac{P_T}{P_O} = \left(1 + \frac{\kappa - 1}{2} M^2\right)^{\frac{\kappa}{\kappa - 1}} \qquad (1)$$

Flow in Region B:

$$\frac{P_1}{P_O} = \frac{A_O}{A_1} \frac{M_O}{M_1} \sqrt{\frac{2 + (\kappa - 1) M_O^2}{2 + (\kappa - 1) M_1^2}} \qquad (2)$$

3.2 Weft traction force

Figure 7 shows the weft traction force against the change of tank pressure for various needle shapes. When the tank pressure is lower than P_T=4 kgf/cm^2, all needles show the same tendency of increasing weft traction force as P_T increases. As P_T becomes 5 kgf/cm^2, we can see a difference in the effect of the needle shape, particularly in model No. 7.

Figure 8 shows the distribution of the weft traction force in the various tank pressures. Even as the weft traction force increases with the increases of tank pressure, strong turbulence will occur when the tank pressure P_T is bigger than 4 kgf/cm^2. Therefore, the optimal driving pressure is 2~4 kgf/cm^2.

3.3 Velocity and turbulence distribution

Figure 9 and figure 10 show the velocity distribution and turbulence intensity at every axial distance for model No. 7. In figure 11, we see that the recirculation zone occurs at axial distance x/D=0.75, reaches the maximum velocity of recirculation at x/D=1.0, and decreases gradually to axial distance x/D=1.75. The flow becomes uniform from x/D=5.0. In figure 12, we can see the location and intensity of the turbulence. It tends to become higher in the recirculation zone and the region around the wall.

Figure 11 and figure 12 show the velocity distribution and turbulence intensity distribution, respectively, for the various needle shapes. In figure 11, we can see that the recirculation zone occurs in model No. 7 and model No. 1. However, as the needle recedes,

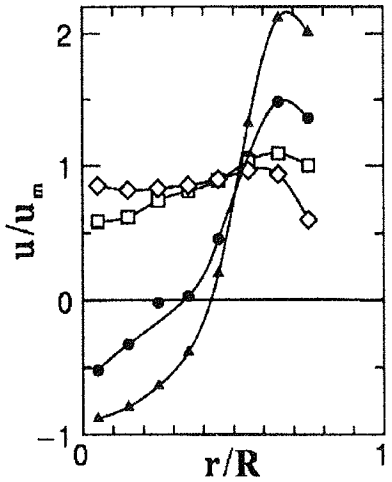

Fig. 11 Velocity distribution along the center

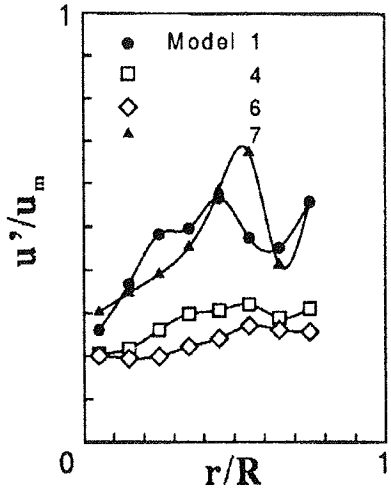

Fig. 12 Turbulence distribution along the center

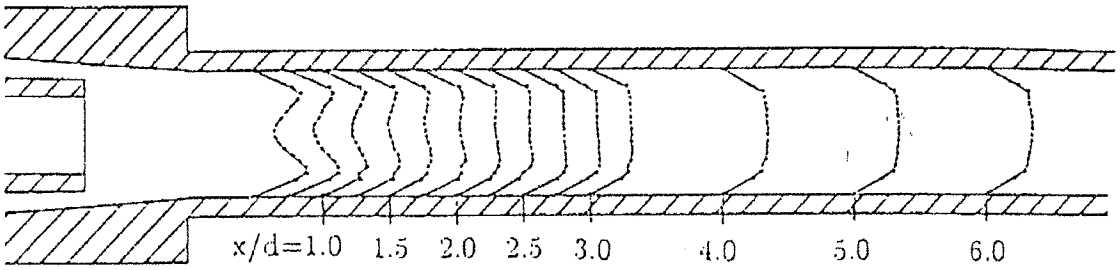

(a) Model No. 4

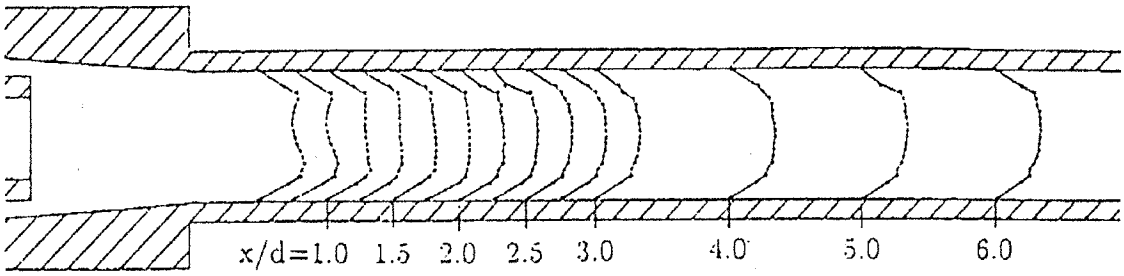

(b) Model No. 6

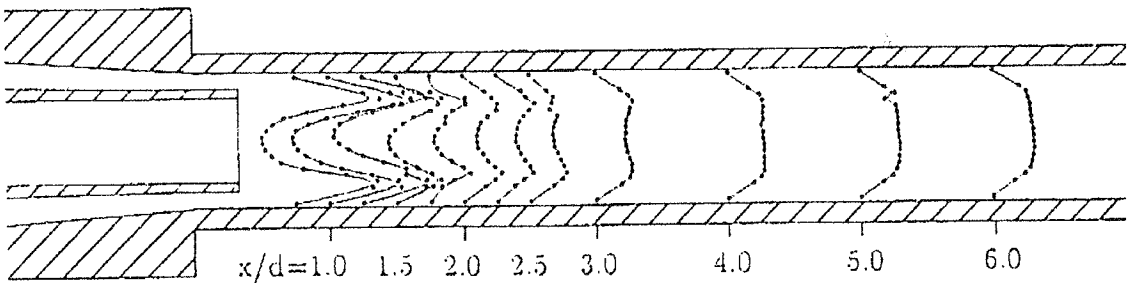

(c) Model No. 7

Fig. 13 Velocity profile along the axial distance (Re=14000)

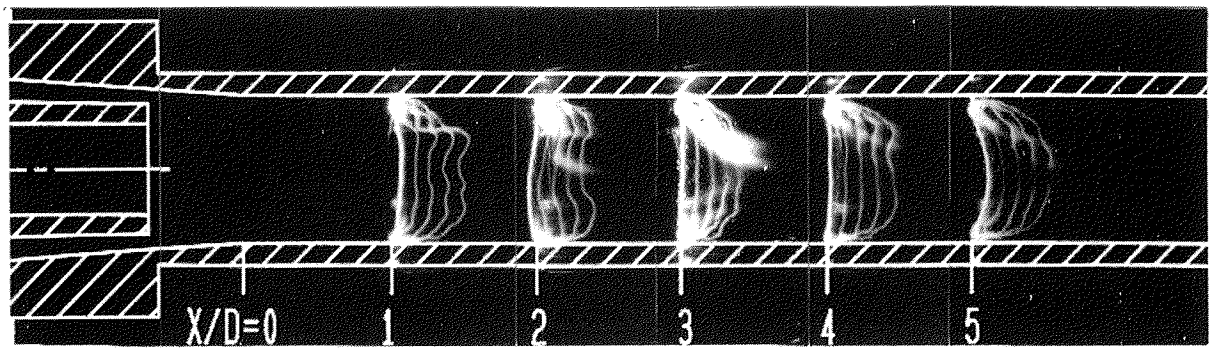

Model 4

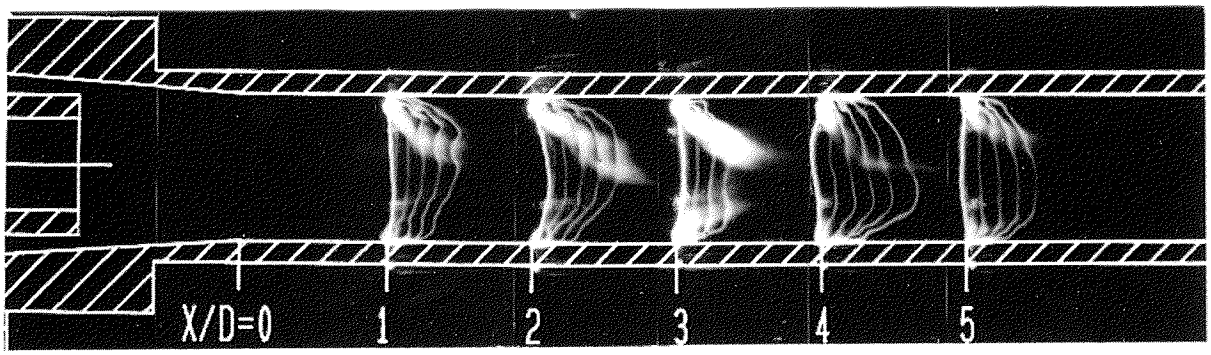

Model 6

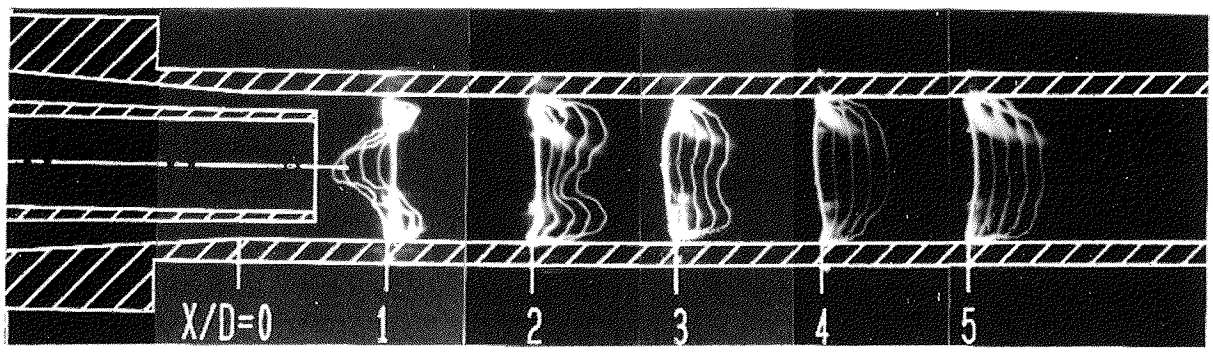

Model 7

Fig. 14 Visualization result (Closed)

we find that flow begins to recover quickly. Also, from figure 12, we see that model No. 1 and model No. 7 have a higher turbulence intensity compared with other models. On the basis of these two figures, we recommend model No. 6, which has low turbulence intensity. Figure 13 shows the velocity distribution in the acceleration tube of nozzle models No. 4, 6 and 7. These three models show different flow patterns along x/D= 1.0~2.0. However, the flow develops gradually and shows the same pattern as axial distance reaches x/D= 5.0~6.0.

3.4 Visualization by spark tracing method

Figure 14 and figure 15 show the visualization results of spark tracing when the tank pressure was P_T=0.5 kgf/cm^2. Both figures show that flow gradually becomes uniform from x/D=5 and also that model No. 6 has a good velocity distribution compared with the others.

In figure 14, when the flow in the needle stops (Closed), we can see that the recirculation zone occurs in model No. 7 at x/D=1.0. Figure 15 shows the visualization of flow in the needle (Open). These results also show a different distribution at x/D=1.0. We consider the cause to be strong turbulence and the high frequency of flow in region B, which exceeds the applicable frequency in the spark tracing method.

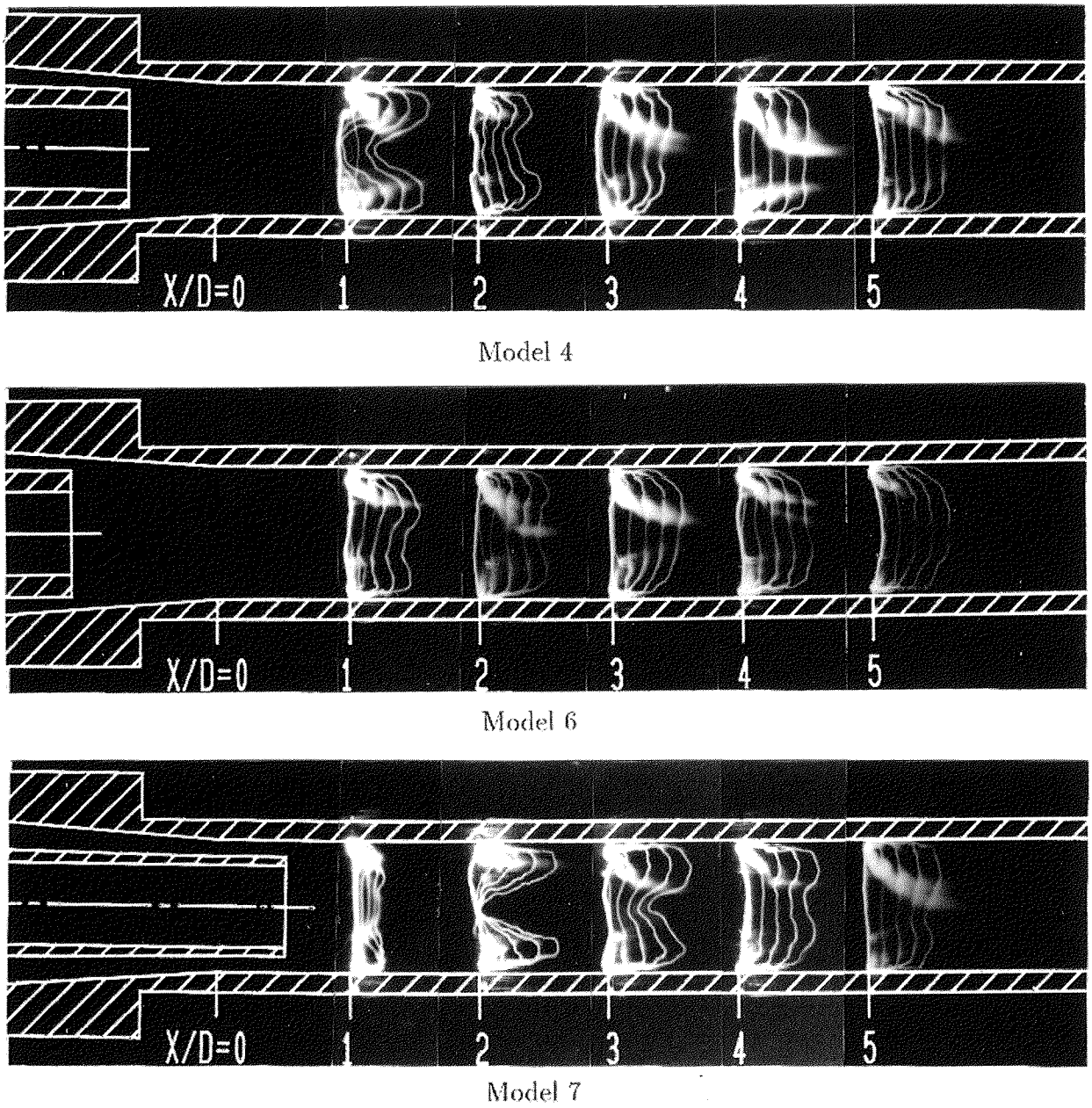

Fig. 15 Visualization result (Open)

4. Conclusions

In this study, the following items were clarified as a result of static pressure and weft traction force measurements, LDV experiment and visualization by the spark tracing method.

1. The weft traction force does not change when tank pressure between P_T=2~4 kgf/cm^2 is applied, for any of the nozzles. As the tank pressure exceeds P_T= 4 kgf/cm^2, the weft traction force of model No. 6 increases faster than those of other models.
2. The recirculation zone occurs in region B along the acceleration tube. From x/D=5, the stalling velocity will decrease and the flow will develop gradually.
3. On withdrawing the needle, the flow begins to recover quickly. Model No. 6 has a low turbulence intensity compared with other models at every axial distance.
4. Since increasing the tank pressure beyond 4 kgf/cm^2 will not improve the static pressure distribution, in order to reduce the turbulence intensity and increase the efficiency, it is better to apply tank pressure P_T between 2~4 kgf/cm^2.

References

[1] Uno, M., A Study on Air Jet Loom with Substream Added, *J. Textile Machine Soc. Jpn*, Vol. 25 (1972) 14-23.

[2] Ishida, M. and Okajima, A., Experimental Study on the Flow

of an Air Jet Loom with an Air Guide, *J. Textile Mechine Soc. Jpn*, Vol. 42 (1989) 63-69.

[3] Ishida, M. and Okajima, A., Flow Characteristics of the Main Nozzle in an Air-Jet Loom Part 1, J. Textile Research, Vol. 64 (1) (1994) 10-20.

[4] Ishida, M. and Okajima, A., Flow Characteristics of Main Nozzle in an Air-Jet Loom Part 2, J. Textile Research, Vol. 64 (2) (1994) 88-100.